

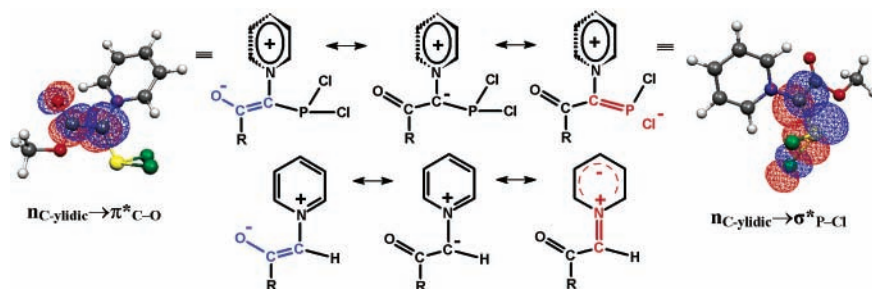
## Substituent-Dependent Anomeric Effects as a Source of Conformational Preference in Pyridinium Methylides

Neelima Gupta,\* Kirti Kr. Shah, and Reena Garg

Department of Chemistry, University of Rajasthan, Jaipur-302 004, India

neelima@sancharnet.in

Received September 2, 2005



A systematic density functional theory level investigation of differently substituted pyridinium methylides was carried out to determine the role of  $C_{ylidic}$  lone-pair-associated hyperconjugative and negative hyperconjugative interactions in deciding conformational preferences. Deviation from the coplanar orientation of the carbanionic center with the pyridine ring and its substituent dependence has been found to correlate well with the relative opportunities for conjugative and negative hyperconjugative interactions of a ylidic moiety with different substituent groups present at the ylidic carbon. The contribution of individual  $n \rightarrow \pi^*$  conjugative,  $n \rightarrow \sigma^*$  negative hyperconjugative, and  $\sigma \rightarrow \pi^*$  hyperconjugative interactions in a particular conformation of pyridinium dichlorophosphinomethylides was assessed from donor–acceptor stabilization energies, as obtained from natural bond orbital (NBO) analysis. The relative extent of conjugative and negative hyperconjugative interactions with the substituents present at the ylidic carbon plays an important role in permitting the delocalization of ylidic charge into the pyridine ring, thereby controlling the relative orientation of the latter with the carbanionic plane.

### Introduction

Cycloiminium ylides are well-known key intermediates in the synthesis of bicyclic azaheterocycles. The greater stabilization of the synthetically important pyridinium-type ylides as compared to the ammonium ylides has been attributed to the delocalization<sup>1</sup> of carbanionic charge into the heterocyclic ring leading to a coplanar orientation of the nearly planar ylidic carbon and the pyridine ring.<sup>2,3</sup> The X-ray structure investigation studies of a number of  $\alpha$ -stabilized pyridinium ylides **1** having an electron-withdrawing substituent ( $Y = \text{CN}, \text{COCl}, \text{COR}, \text{NO}_2$ , etc.) on the ylidic carbon,<sup>4–8</sup> however, revealed that the relative orientation of the plane of the pyridine ring and the

carbanionic center varies to a great extent from nearly coplanar to almost perpendicular and requires an explanation. Recently, several theoretical studies<sup>3,9–12</sup> of the pyridinium methylides have appeared in the literature where the results have been found

(1) Johnson, A. W. *Ylide Chemistry*; Academic Press: New York, 1996; p 260.

(2) Bugg, C.; Desiderato, R.; Sass, R. L. *J. Am. Chem. Soc.* **1964**, *86*, 3157.

(3) Karzazi, Y.; Surpateanu, G.; Lungu, C. N.; Vergoten, G. *J. Mol. Struct.* **1997**, *406*, 45.

(4) Ning, R. Y.; Madan, P. V.; Blount, J. F.; Fryer, R. I. *J. Org. Chem.* **1976**, *41*, 3406.

(5) Bailey, N. A.; Newton, G. G. *Cryst. Struct. Commun.* **1980**, *9*, 49.

(6) Wittmann, H.; Ziegler, E.; Peters, K.; Peters, E. M.; von Schnering, H. G. *Monatsh. Chem.* **1983**, *114*, 1097.

(7) Banks, R. E.; Pritchard, R. G.; Thomson, J. J. *Chem. Soc., Perkin Trans. I* **1986**, 1769.

(8) Alvarez-Builla, J.; Galvez, E.; Cuadro, A. M.; Florencio, F.; Garcia-Blanco, S. *J. Heterocycl. Chem.* **1987**, *24*, 917.

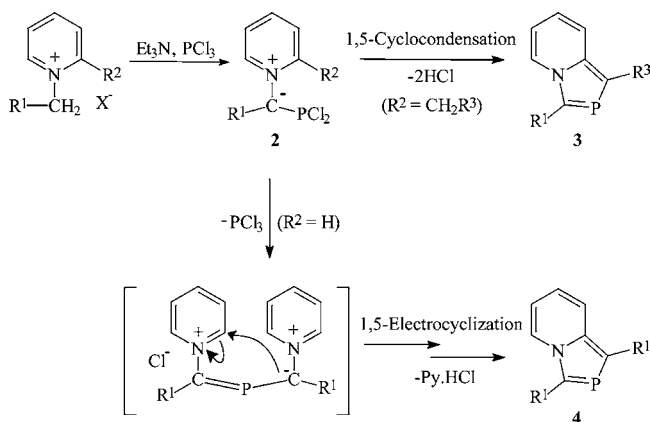
(9) Lledós, A.; Carbó, J. J.; Navarro, R.; Serrano, E.; Urriolabeitia, E. *P. Inorg. Chem.* **2004**, *43*, 7622.

(10) Karzazi, Y.; Vergoten, G.; Surpateanu, G. *J. Mol. Struct.* **1999**, *476*, 121.

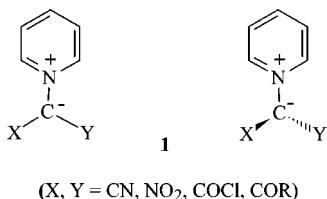
(11) Dega-Szafran, Z.; Schroeder, G.; Szafran, M.; Szwajca, A.; Łęska, B.; Lewandowska, M. *J. Mol. Struct.* **2000**, *555*, 31.

(12) Bonneau, R.; Collado, D.; Dalibart, M.; Liu, M. T. H. *J. Phys. Chem. A* **2004**, *108*, 1312.

## SCHEME 1



to be in good agreement with the experimental geometries, and in a few cases,<sup>9,10</sup> the spatial arrangement of two moieties has also been addressed. In  $\alpha$ -keto stabilized ylides, the observed noncoplanarity has been assigned to the presence of a 1,4-N $\cdots$ O interaction, whereas the stabilization of a coplanar conformation in other cases has been attributed to the presence of 1,6-C–H $\cdots$ O hydrogen bonding.<sup>9</sup> In a comparative molecular field analysis study of differently substituted pyridinium methylides, the deviation from coplanarity has been correlated to the cumbersomeness of the substituent present on the ylidic carbon.<sup>10</sup>



In analogy with the intermediacy of pyridinium methylides in the synthesis of bicyclic azaheterocycles such as indolizines and related systems,<sup>13</sup> we isolated the intermediate pyridinium dichlorophosphinomethylides<sup>14–17</sup> **2** during the synthesis of 2-phosphaindolizines (**3** and **4**) (Scheme 1); the latter represents a novel class of bicyclic azaheterocycles incorporating a  $\sigma^2, \lambda^3$ -phosphorus as an additional heteroatom in the five-membered ring. Semiempirical PM3 calculations<sup>18</sup> of a few representative pyridinium dichlorophosphinomethylides resulted in the minimum energy geometries representing a coplanar orientation of the pyridinium ring and the carbanionic plane, similar to an earlier observation made from theoretically calculated geometries of the nonphosphorus analogues.<sup>11</sup> We subsequently investigated the X-ray crystal structure of 2-ethylpyridinium dichlorophosphino-ethoxycarbonylmethylide **2** ( $R^1 = \text{CO}_2\text{Et}$ ,

$R^2 = \text{Et}$ ).<sup>19</sup> Two characteristic structural features were observed: (1) the unsymmetrical disposition of the  $\text{PCl}_2$  group around the carbanionic plane and (2) unequal lengths of the two P–Cl bonds (208.98(10) and 217.78(13) Å), which were recognized to be a consequence of the presence of  $n_{\text{C}_{\text{ylidic}}} \rightarrow \sigma^*_{\text{P-Cl}}$  negative hyperconjugative interactions. Another structural feature, i.e., the noncoplanarity of the pyridinium ring and the carbanionic center in **2**, is of special interest in the context of generalized pyridinium methylides and deserves further investigation.

Theoretical ab initio and DFT calculations of a variety of ylides<sup>20–25</sup> and related species<sup>26–31</sup> have been reported to explain their structure, bonding, or internal rotational processes. In a number of cases, the importance of the  $\pi \rightarrow \sigma^*$  or  $n \rightarrow \sigma^*$  anomeric effects, now more generally termed *negative hyperconjugation*,<sup>32,33</sup> in understanding conformational preferences has been pointed out.<sup>27–31</sup> The natural bond orbital (NBO) approach of Weinhold et al.<sup>34</sup> has been frequently used to quantify the substituent dependence of hyperconjugation<sup>35,36</sup> as well as negative hyperconjugation<sup>37–41</sup> within the context of conformational analysis. Reports on the theoretical investigations on how the hyperconjugative and related interactions influence the structural parameters in the pyridinium ylides are, however, still scarce, and the main goal of this work is to highlight the influence of such interactions on the conformational preferences of these synthetically important intermediates.

During the present study, with an aim to investigate the effect of various substituents at the ylidic carbon on the extent of negative hyperconjugation in different rotamers of pyridinium dichlorophosphinomethylides resulting in experimentally observed conformational preferences, we have found that it is the relative strengths of the carbanionic lone-pair-associated  $n \rightarrow \pi^*$  conjugative and  $n \rightarrow \sigma^*$  negative hyperconjugative interactions to the two substituents of the ylidic center that prevent or allow the resonance delocalization of the ylidic charge into the pyridine

(19) Bansal, R. K.; Gupta, N.; Singh, S.; Karaghiosoff, K.; Mayer, P.; Vogt, M. *Tetrahedron Lett.* **2004**, *45*, 7771.

(20) Nyulászai, L.; Veszprémi, T. *J. Phys. Chem.* **1996**, *100*, 6456.

(21) Naito, T.; Nagase, S.; Yamataka, H. *J. Am. Chem. Soc.* **1994**, *116*, 10080.

(22) Dobado, J. A.; Martínez-García, H.; Molina, J. M.; Sundberg, M. R. *J. Am. Chem. Soc.* **2000**, *122*, 1144.

(23) Bachrach, S. M. *J. Org. Chem.* **1992**, *57*, 4367.

(24) Lledós, A.; Carbo, J. J.; Urriolabeitia, E. P. *Inorg. Chem.* **2001**, *40*, 4913.

(25) Karafiloglou, P.; Harcourt, R. D. *J. Mol. Struct. (TheoChem)* **2005**, *729*, 165.

(26) Cramer, C. J.; Denmark, S. E.; Miller, P. C.; Dorow, R. L.; Swiss, K. A.; Wilson, S. R. *J. Am. Chem. Soc.* **1994**, *116*, 2437.

(27) Raabe, G.; Gais, H.-J.; Fleischhauer, J. *J. Am. Chem. Soc.* **1996**, *118*, 4622.

(28) Wiberg, K. B.; Castejon, H. *J. Am. Chem. Soc.* **1994**, *116*, 10489.

(29) Kormos, B. L.; Cramer, C. J. *Inorg. Chem.* **2003**, *42*, 6691.

(30) Bharatam, P. V.; Uppal, P.; Amita; Kaur, D. *J. Chem. Soc., Perkin Trans.* **2000**, *2*, 43.

(31) Bors, D. A.; Streitwieser, A., Jr. *J. Am. Chem. Soc.* **1986**, *108*, 1397.

(32) Schleyer, P. v. R.; Kos, A. J. *Tetrahedron* **1983**, *39*, 1141.

(33) Reed, A. E.; Schleyer, P. v. R. *J. Am. Chem. Soc.* **1990**, *112*, 1434.

(34) Reed, A. E.; Curtis, L. A.; Weinhold, F. *Chem. Rev.* **1988**, *88*, 899.

(35) Bocca, C. C.; Pontes, R. M.; Basso, E. A. *J. Mol. Struct. (TheoChem)* **2004**, *710*, 105.

(36) Alabugin, I. V. *J. Org. Chem.* **2000**, *65*, 3910.

(37) Reed, A. E.; Schleyer, P. v. R. *J. Am. Chem. Soc.* **1987**, *109*, 7362.

(38) Tormena, C. F.; Rittner, R.; Contreras, R. H.; Peralta, J. E. *J. Phys. Chem. A* **2004**, *108*, 7762.

(39) Hetényi, A.; Martinek, T. A.; Lázár, L.; Zalán, Z.; Fülöp, F. *J. Org. Chem.* **2003**, *68*, 5705.

(40) Mo, Y.; Zhang, Y.; Gao, J. *J. Am. Chem. Soc.* **1999**, *121*, 5737.

(41) Chuang, C.-H.; Lien, M.-H. *J. Phys. Chem. A* **2004**, *108*, 1790.

(13) Bansal, R. K.; Gupta, N.; Surana, A. *J. Indian Chem. Soc.* **1998**, *75*, 648.

(14) Bansal, R. K.; Karaghiosoff, K.; Gupta, N.; Schmidpeter, A.; Spindler, C. *Chem. Ber.* **1991**, *124*, 475.

(15) Bansal, R. K.; Gupta, N.; Gupta, R.; Pandey, G.; Agarwal, M. *Phosphorus Sulfur Silicon* **1996**, *112*, 121.

(16) Bansal, R. K.; Surana, A.; Gupta, N. *Tetrahedron Lett.* **1999**, *40*, 1565.

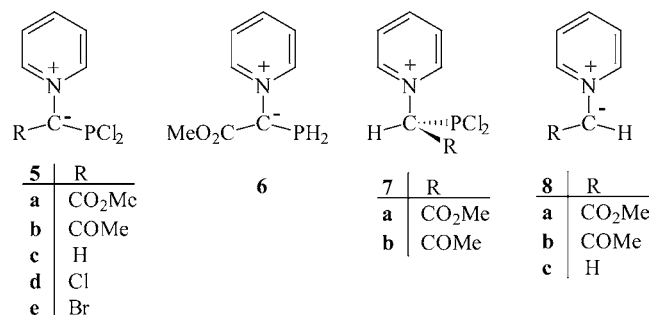
(17) Bansal, R. K.; Gupta, N.; Baweja, M.; Hemrajani, L.; Jain, V. K. *Heteroat. Chem.* **2001**, *12*, 602.

(18) Bansal, R. K.; Gupta, N.; Bansal, S. *Indian J. Chem.* **2004**, *43B*, 144.

ring, thereby affecting the coplanarity in question. To explain these observations, we present in this paper a systematic quantum chemical study of conformational analyses of differently substituted pyridinium dichlorophosphinomethylides (**5**) and related systems (**6** and **7**) at the density functional theory (DFT) level. The location of minima on the rotational coordinate has been found to be dependent on the opportunities for conjugative or negative hyperconjugative interactions, which are reflected in structural features such as C–P bond shortening, P–Cl bond elongation, and coplanarity of the ylidic carbon with the pyridinium ring along with the partial atomic charges on participating atoms. An important point to be noted is the variation in coplanarity of the carbanionic center and the pyridinium ring on changing the ylidic substituent in pyridinium dichlorophosphinomethylide or on replacing the  $\text{PCl}_2$  moiety with  $\text{PH}_2$  or H. Natural bond orbital analysis has been, therefore, applied to identify main orbital interactions to rationalize the effect of substituents on the extent of negative hyperconjugative and other conjugative interactions in a particular conformer. The effect of solvation on rotational barrier lowering has also been estimated.

### Computational Methods

The Gaussian 98W package<sup>42</sup> was used to carry out all calculations. Potential energy surfaces were built using the restricted Hartree–Fock (RHF) method along with the 6-31G basis set for the ylides **5a,b** and **6** in the context of C–P bond rotation. The stable low energy conformers, as well as the high energy saddle points connecting them, were optimized at the density functional (DFT) level of theory<sup>43</sup> using the B3LYP hybrid functional<sup>44</sup> by applying the 6-311G\*\* basis set. The stationary points thus optimized were characterized by frequency calculations to verify that the true minima and the transition structures have zero and one imaginary frequency, respectively. The geometries of the rotamers corresponding to the most stable minimum of pyridinium ylides **5c–e** and **8a–c** and the pyridinium ions **7a,b** have also been optimized at the same level and verified by frequency calculations through vibrational analysis. Diffuse functions have been included by carrying out single-point energy calculations (B3LYP/6-311++G\*\* level) of the B3LYP/6-311G\*\* level optimized geometries,<sup>45</sup> and to the single-point energies thus obtained, unscaled zero-point vibrational energy corrections (ZPE) from B3LYP/6-311G\*\* level frequency calculations have been applied (Table 1).



The electronic structure of the most stable rotamer in each case was studied using NBO analysis.<sup>46–48</sup> Stabilization energies associated with donor–acceptor interactions, reflecting the presence of delocalization, hyperconjugation, and negative hyperconjugation, were estimated from second-order perturbation analysis of the Fock matrix on NBO basis. NBO calculations were performed at the B3LYP/6-311++G\*\* level on B3LYP/6-311G\*\* optimized ge-

**TABLE 1.** Relative Energies of Different Rotamers of **5a**, **5b**, and **6**

|                         | $N_{\text{imag}}$ | relative energies (kcal/mol) <sup>a</sup> |       |
|-------------------------|-------------------|---|-------|
| <b>5aM1</b>             | 0                 | 0.0                                       | 0.0   |
| <b>5aM2</b>             | 0                 | 6.06                                      | 6.10  |
| <b>5aM2<sup>b</sup></b> |                   | 5.66                                      | 5.64  |
| <b>5aM2<sup>c</sup></b> |                   | 5.19                                      | 4.90  |
| <b>5aTS<sub>a</sub></b> | 1                 | 12.45                                     | 11.95 |
| <b>5aTS<sub>b</sub></b> |                   | 11.92                                     | 11.35 |
| <b>5aTS<sub>c</sub></b> |                   | 10.74                                     | 10.26 |
| <b>5bM1</b>             | 0                 | 0.0                                       | 0.0   |
| <b>5bM2</b>             | 0                 | 5.21                                      | 5.35  |
| <b>5bTS</b>             | 1                 | 11.81                                     | 11.51 |
| <b>6M1</b>              | 0                 | 0.0                                       | 0.0   |
| <b>6M2</b>              | 0                 | 0.099                                     | 0.17  |
| <b>6TS</b>              | 1                 | 3.30                                      | 3.19  |

<sup>a</sup> Values in the first column at the B3LYP/6-311G\*\*/B3LYP/6-311G\*\* level, and those in the second column at the B3LYP/6-311++G\*\*/B3LYP/6-311G\*\* level. <sup>b</sup> In toluene. <sup>c</sup> In dichloromethane; all other values were calculated in the gas phase.

ometries using the NBO 3.1 module,<sup>49</sup> as implemented in Gaussian 98W. The overlapping NBO orbitals were visualized with the molecular graphics package MOLEKEL.<sup>50</sup> Solvent effects were taken into account by B3LYP/6-311++G\*\* level single-point calculations of the stationary points optimized in solvent at the B3LYP/6-311G\*\* level using the self-consistent reaction field (SCRF)<sup>51</sup> method based on Tomasi's polarizable continuum model (PCM),<sup>52</sup> in which the atomic radii from the simple united atom topological model are used to build the cavity. The dielectric constants at 298.0 K,  $\epsilon = 8.93$ , and 2.379 have been used for dichloromethane and toluene, respectively.

### Results and Discussion

**Conformational Analysis.** Figure 1 depicts the potential energy profile for rotation around the C7–P8 bond of pyridinium dichlorophosphinomethylides **5a** and **5b** along with the atom numbering used for further discussion. For each molecule,

(42) Frisch, M. J.; Trucks, G. W.; Schlegel, H. B.; Scuseria, G. E.; Robb, M. A.; Cheeseman, J. R.; Zakrzewski, V. G.; Montgomery, J. A., Jr.; Stratmann, R. E.; Burant, J. C.; Dapprich, S.; Millam, J. M.; Daniels, A. D.; Kudin, K. N.; Strain, M. C.; Farkas, O.; Tomasi, J.; Barone, V.; Cossi, M.; Cammi, R.; Mennucci, B.; Pomelli, C.; Adamo, C.; Clifford, S.; Ochterski, J.; Petersson, G. A.; Ayala, P. Y.; Cui, Q.; Morokuma, K.; Malick, D. K.; Rabuck, A. D.; Raghavachari, K.; Foresman, J. B.; Cioslowski, J.; Ortiz, J. V.; Stefanov, B. B.; Liu, G.; Liashenko, A.; Piskorz, P.; Komaromi, I.; Gomperts, R.; Martin, R. L.; Fox, D. J.; Keith, T.; Al-Laham, M. A.; Peng, C. Y.; Nanayakkara, A.; Gonzalez, C.; Challacombe, M.; Gill, P. M. W.; Johnson, B. G.; Chen, W.; Wong, M. W.; Andres, J. L.; Head-Gordon, M.; Replogle, E. S.; Pople, J. A. *Gaussian 98*, revision A.11.4; Gaussian, Inc.: Pittsburgh, PA, 2002.

(43) (a) Parr, R. G.; Yang, W. *Density Functional Theory of Atoms and Molecules*; Oxford University Press: New York, 1989. (b) Ziegler, T. *Chem. Rev.* **1991**, *91*, 651.

(44) (a) Becke, A. D. *J. Chem. Phys.* **1993**, *98*, 5648. (b) Lee, C.; Yang, W.; Parr, R. G. *Phys. Rev. B* **1998**, *37*, 785.

(45) Optimization of one representative (**5aM1**) has been done at the B3LYP/6-311++G\*\* level also to ensure that the influence of the presence of diffuse functions on the optimized geometrical parameters is negligible (see Supporting Information Tables SI-2 and SI-3).

(46) Foster, J. P.; Weinhold, F. *J. Am. Chem. Soc.* **1980**, *102*, 7211.

(47) Reed, A. E.; Weinstock, R. B.; Weinhold, F. *J. Chem. Phys.* **1985**, *83*, 785.

(48) Reed, A. E.; Weinhold, F. *J. Chem. Phys.* **1985**, *83*, 1736.

(49) Glending, E. D.; Reed, A. E.; Carpenter, J. E.; Weinhold, F. *NBO version 3.1*, as implemented in *Gaussian 98*.

(50) (a) Flükiger, P.; Lüthi, H. P.; Portmann, S.; Weber, J. *MOLEKEL 4.3*; Swiss Center for Scientific Computing: Manno, Switzerland, 2000–2002. (b) Portmann, S.; Lüthi, H. P. *Chimia* **2000**, *54*, 766.

(51) Tomasi, J.; Persico, M. *Chem. Rev.* **1994**, *94*, 2027.

(52) Cancas, E.; Mennucci, B.; Tomasi, J. *J. Chem. Phys.* **1997**, *107*, 3032.

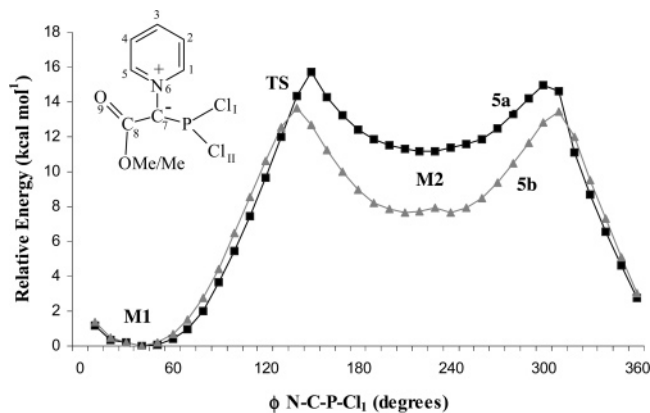


**FIGURE 1.** Potential energy surface (RHF/6-31G level) for rotation around the C7–P bond in **5a** and **5b**.

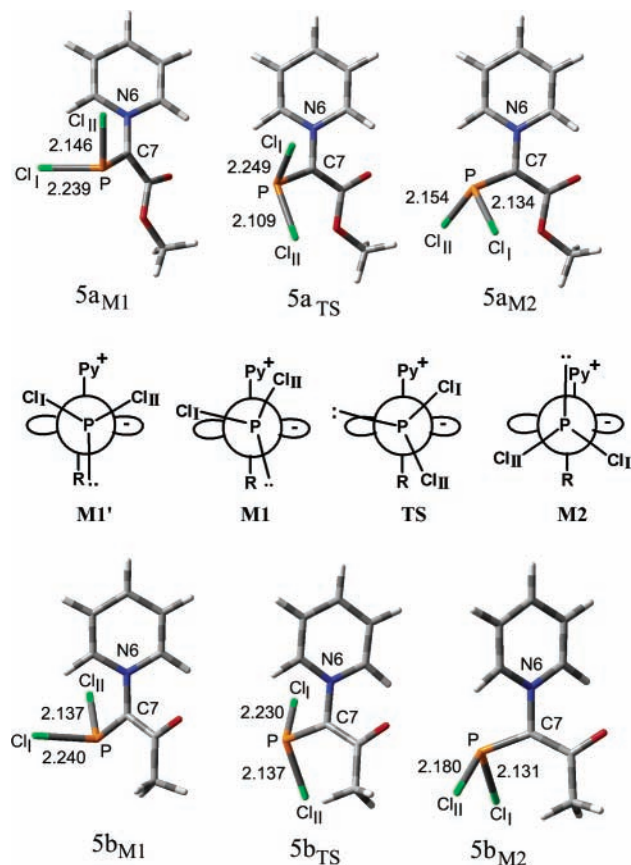


**FIGURE 2.** B3LYP/6-311G\*\* optimized geometries and Newman projections of minimum energy rotamers **5a<sub>M1</sub>**, **5a<sub>M2</sub>**, **5b<sub>M1</sub>**, and **5b<sub>M2</sub>** and saddle points **5a<sub>TS</sub>** and **5b<sub>TS</sub>**.

two minima separated by a substantial energy gap could be located on the rotational hypersurface.

The optimized geometries of the two minima in each case (**5a<sub>M1</sub>** and **5a<sub>M2</sub>** and **5b<sub>M1</sub>** and **5b<sub>M2</sub>**) and the corresponding saddle points (**5a<sub>TS</sub>** and **5b<sub>TS</sub>**) connecting them calculated at the B3LYP/6-311G\*\* level are presented in Figure 2.

Stability of different rotamers of pyridinium dichlorophosphinomethylides, incorporating a planar ylidic sp<sup>2</sup> carbon (sum of the three angles on C7 ≈ 360°; Supporting Information Table SI-2) and a pyramidal sp<sup>3</sup> phosphorus, may be perceived as being dependent on the relative orientation of the ylidic charge and the phosphorus lone pair. Orthogonal orientation of the two

lone pairs minimizes their repulsive interaction, thereby stabilizing that particular conformation. Accordingly, a higher energy minimum (**5a<sub>M2</sub>** and **5b<sub>M2</sub>**) corresponds to the conformer having almost a synperiplanar orientation of the pyridine ring and the phosphorus lone pair ( $\phi$  N–C–P–Cl<sub>I</sub> = 135.1°, 141.3°;  $\phi$  N–C–P–Cl<sub>II</sub> = 121.7°, 116.7°), as represented by the Newman projection formula **M<sub>2</sub>** (Figure 2). The conformation of the global minimum in each case (**5a<sub>M1</sub>** and **5b<sub>M1</sub>**), however, deviates much from the expected antiperiplanar orientation **M<sub>1</sub>'** and exhibits one chlorine atom in nearly orthogonal orientation ( $\phi$  N–C–P–Cl<sub>I</sub> ≈ 70°) with respect to the pyridine ring (Newman projection **M<sub>1</sub>**, i.e., the P–Cl<sub>I</sub> bond eclipsed by the p<sub>z</sub> orbital of the ylidic carbon), which is in good accordance with the experimentally observed geometry of 2-ethylpyridinium dichlorophosphino-ethoxycarbonylmethylide.<sup>19</sup> Furthermore, the calculated geometries reveal that the plane of the pyridine ring and that of the carbanionic center are not coplanar ( $\phi$  C5–N6–C7–P = 129–136°), which should otherwise give an extra stabilization as a result of the extended delocalization of the ylidic charge into the pyridine ring as well as the C=O moiety of the C<sub>ylidic</sub> substituent. These deviations can be rationalized by the presence of negative hyperconjugative interactions between n<sub>C<sub>ylidic</sub></sub> and σ\*<sub>P–Cl<sub>I</sub></sub> orbitals facilitated by their parallel orientation. The observed noncoplanarity of the plane of the C7 carbon and the pyridine ring further increases the availability of the ylidic charge for the n<sub>C<sub>ylidic</sub></sub> → σ\*<sub>P–Cl<sub>I</sub></sub> interaction as a result of the reduced extent of delocalization of the ylidic electrons into the pyridine ring, as explained later by NBO calculations.

The saddle point on the rotational hypersurface (characterized by  $N_{\text{imag}} = 1$ ; the imaginary frequency corresponding to rotational motion about the C7–P bond) corresponds to ~90° torsion about the C7–P bond relative to **M<sub>2</sub>** so that the two lone pairs have almost parallel orientation (Newman projection **TS**; Figure 2) causing a maximum destabilizing interaction.

The existence of negative hyperconjugation in a particular conformer is manifested by several features such as a lowering in potential energy, bond elongation at the acceptor site with concomitant bond shortening at the donor site, and charge transfer.<sup>32,37,40</sup>

At the B3LYP/6-311G\*\* level, the minimum energy rotamers **5a<sub>M1</sub>** and **5b<sub>M1</sub>**, having conformations favorable to permit n<sub>C<sub>ylidic</sub></sub> → σ\*<sub>P–Cl</sub> negative hyperconjugative interactions, are more stable than the higher energy minima **5a<sub>M2</sub>** and **5b<sub>M2</sub>** by 6.06 and 5.21 kcal/mol, respectively, and are separated by a substantial rotational barrier of 12.45 and 11.81 kcal/mol (Table 1). Inclusion of the diffuse functions in single-point calculations (B3LYP/6-311++G\*\* level) at the B3LYP/6-311G\*\* optimized geometries increases the energy gap between two minima slightly, and the rotational barriers are somewhat lowered. The solvent effect for the presence of toluene and dichloromethane has been calculated for **5a** by B3LYP/6-311G\*\* optimizations of **5a<sub>M1</sub>**, **5a<sub>M2</sub>**, and **5a<sub>TS</sub>** followed by single-point energy calculations at the B3LYP/6-311++G\*\* level. Solvent interactions stabilize each of the two minima as well as the transition state, with the stabilization being in the order **TS** > **M<sub>2</sub>** > **M<sub>1</sub>**, resulting in a reduced rotational barrier and a smaller difference in the energy of the two minima (Table 1); the effect of the presence of dichloromethane is more in magnitude.

To account for the extra stabilization of the conformation **M<sub>1</sub>** and high rotational barriers due to the presence of negative hyperconjugation in pyridinium dichlorophosphinomethylides **5a** and **5b**, we have selected pyridinium methoxycarbonyl-

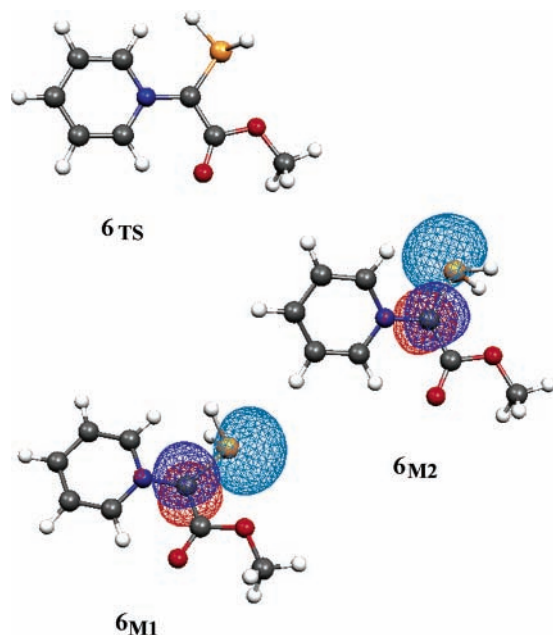


**FIGURE 3.** B3LYP/6-311G\*\* optimized geometries of **6M1**, **6M2**, and **6TS** illustrating orthogonal orientation of the anionic charge and the lone pair on phosphorus in **6M1** and **6M2**.

phosphinomethylide **6** as the model compound in which the extent of negative hyperconjugation reduces substantially due to the P–H bond being a much weaker acceptor site as compared to the P–Cl bond for the donation of the  $C_{\text{ylidic}}$  charge. The rotational hypersurface of **6** about the C7–P bond shows the presence of two minima **6M1** and **6M2** of almost equal energy ( $\Delta E < 0.2$  kcal/mol) separated by a saddle point **6TS** having a rotational barrier of only 3.19 kcal/mol. In this case, the optimized geometries of both minima (**6M1** and **6M2**, Figure 3) illustrate the relative disposition of the  $C_{\text{ylidic}}$  electrons and the phosphorus lone pair to be orthogonal, causing minimum interaction leading to similar stabilization. Because both **6M1** and **6M2** are not significantly stabilized by negative hyperconjugation, their rotational barrier is quite small.

The bond lengths within the  $>C^--PCl_2$  moiety of **5a** and **5b** are affected strongly by the presence of an  $n_{C_{\text{ylidic}}}\rightarrow\sigma^*_{P-Cl}$  hyperconjugative effect, and a comparison of these bond distances with those in the corresponding pyridinium ions **7a** and **7b** (Figure 4), in which the  $n_{C_{\text{ylidic}}}\rightarrow\sigma^*_{P-Cl}$  negative hyperconjugation is absent, provides a measure of its magnitude. As compared to the pyridinium ions **7a** and **7b**, P–Cl bond lengths in the corresponding ylides **5a** and **5b** become longer; elongation is larger ( $\sim 15$  pm) for P–Cl<sub>I</sub> in **M1** and is accompanied by a significant decrease ( $\sim 18$  pm) in the distance and increase in the bond order of the C7–P bond (Supporting Information Table SI-3). Thus, the lengthening of the P–Cl<sub>I</sub> bond by  $\sim 10$  pm in comparison to the P–Cl<sub>II</sub> bond in **5aM1** and **5bM1** accompanied by an enhancement of the negative charge on Cl<sub>I</sub> is attributable to the  $n_{C_{\text{ylidic}}}\rightarrow\sigma^*_{P-Cl}$  interaction. In the absence of any significant charge transfer from ylidic carbon to any of the  $\sigma^*_{P-H}$  orbitals in **6**, the two P–H bond lengths are almost equal and the C7–P distance is longer by  $\sim 6$  pm as compared to that in **5a,b** (Supporting Information Table SI-3). Similar geometrical effects have been found in a number of theoretical investigations supporting negative hyperconjugation.<sup>26–29,32,53</sup>

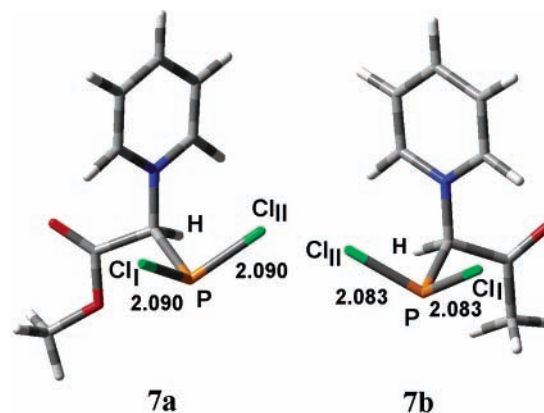


**FIGURE 4.** B3LYP/6-311G\*\* optimized geometries of pyridinium ions **7a** and **7b**.

Interestingly, the P–Cl<sub>I</sub> bond length in transition structures **5aTS** and **5bTS** has also been found to be elongated which is, however, accompanied by the lengthening of the C7–P distance with a simultaneous decrease in bond order. These structural features in the transition states can be rationalized by the presence of  $\sigma_{P-Cl}\rightarrow\pi^*_{C7-P}$  hyperconjugative interactions in addition to  $\pi_{C7-P}\rightarrow\sigma^*_{P-Cl}$  interactions, as evident from NBO analysis given later.

Because the stability of **5a** in solution was previously reported to be dependent on the nature of the solvent,<sup>15,16</sup> optimizations of **5aM1**, **5aM2**, and **5aTS** have been done in toluene and dichloromethane also. The C7–P and two P–Cl bond lengths as well as the charges on chlorine atoms thus obtained (Supporting Information Table SI-3) indicate that the extent of negative hyperconjugation increases only slightly in toluene. However, the presence of polar solvent such as dichloromethane enhances the  $n_{C_{\text{ylidic}}}\rightarrow\sigma^*_{P-Cl}$  interaction considerably, when the difference in two P–Cl bond lengths in **M1** further increases. A much longer P–Cl<sub>I</sub> bond length (2.358 Å) and a large negative partial charge ( $-0.524$ ) on Cl<sub>I</sub> explain the observed disproportionation of **5a**.<sup>16,17</sup>

#### Effect of Substituents at Ylidic Carbon and Coplanarity.

The strength of the negative hyperconjugative interactions has been reported to be affected by the electron-withdrawing effects of the substituent group by altering polarization along the acceptor bond.<sup>27,39</sup> To investigate the influence of different substituents at the ylidic carbon on the conformational preferences and the extent of negative hyperconjugation in pyridinium dichlorophosphinomethylides, the rotamers corresponding to most stable minimum **M1** of **5c–e** have also been optimized (Figure 5). In contrast to **5a** and **5b**, pyridinium dichlorophosphinomethylide **5c** shows conformational preferences similar to that in **6M1**; a perfectly planar ylidic carbon (sum of three angles at C7 =  $360^\circ$ ) is almost coplanar with the pyridine ring ( $\phi$  C5–N6–C7–H =  $0.37^\circ$ ). The symmetrical disposition of the  $-PCl_2$  moiety around the molecular plane ( $\phi$  N6–C7–P–Cl<sub>I</sub>  $\approx$   $\phi$  N6–C7–P–Cl<sub>II</sub>  $\approx$   $49.7^\circ$ ) and two identical P–Cl distances with a comparatively smaller bond order (0.79) are indicative of the presence of  $C_{\text{ylidic}}-P-Cl$  interactions of the same order for the two P–Cl bonds.

On moving from **5c** to **5d** and further to **5e**, by changing the substituent on ylidic carbon to Cl and Br, respectively, the difference between the P–Cl<sub>I</sub> and P–Cl<sub>II</sub> bond lengths and the

(53) Ignacio, E. W.; Schlegel, H. B. *J. Phys. Chem.* **1992**, *96*, 5830.

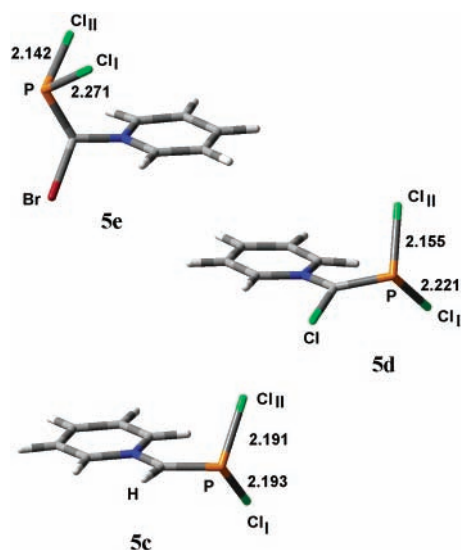


FIGURE 5. B3LYP/6-311G\*\* optimized geometries of **5c–e**.

deviation from the coplanarity ( $\phi$  C5–N6–C7–Cl = 19.7°;  $\phi$  C5–N6–C7–Br = 47.6°) and from the symmetrical disposition of the  $-\text{PCl}_2$  moiety become larger, like those in **5a** and **5b**. In view of these observations, a relationship between substituent-dependent loss of coplanarity and preference of negative hyperconjugative interactions in pyridinium dichlorophosphinomethylides can be inferred. However, it is still not obvious whether it is the mere presence of electron-withdrawing substituents (having either an  $-I$  or  $-M$  effect) at the ylidic carbon or the opportunity of uneven distribution of the ylidic charge into antibonding P–Cl orbitals through negative hyperconjugation that accounts for the diminished delocalization of the carbanionic charge into the pyridine ring leading to the loss of coplanarity. For this purpose, computations of the pyridinium methylides **8a** and **8b**, obtained by replacing the  $-\text{PCl}_2$  moiety of **5a** and **5b** by H, and the unsubstituted pyridinium methylide **8c** have been performed. Optimized geometries in each case (Figure 6) show a perfectly coplanar orientation of the ylidic carbon and the pyridine ring ( $\phi$  C5–N6–C7–C8/H = 0°) which has been previously<sup>9,11</sup> assigned to the presence of 1,6-C–H $\cdots$ O interactions. Although, the O $\cdots$ H distances of 2.03 and 1.96 Å in **8a** and **8b**, respectively, are much smaller than 2.72 Å (the sum of van der Waals radii<sup>54</sup>), they are not accompanied by any significant elongation of the respective C–H and C=O bond lengths as compared to those in **5a** and **5b**. Thus, it is the effective delocalization of the ylidic charge into the pyridine ring which makes the two moieties coplanar in **8a** and **8b**, and the small O $\cdots$ H distances result because of the particular conformation and not because of the 1,6-C–H $\cdots$ O hydrogen bonding. Therefore, it can be concluded that it is not the mere presence of an electron-withdrawing substituent on the ylidic carbon that causes loss of coplanarity, but its presence makes the negative hyperconjugative interactions of the ylidic charge with the  $-\text{PCl}_2$  moiety effective leading to the deviation from coplanarity in question.

**NBO Analysis.** Table 2 lists the stabilization energies  $\Delta E_{ij}$ <sup>55</sup> of some important delocalizations associated with the  $>\text{C}^-$ –

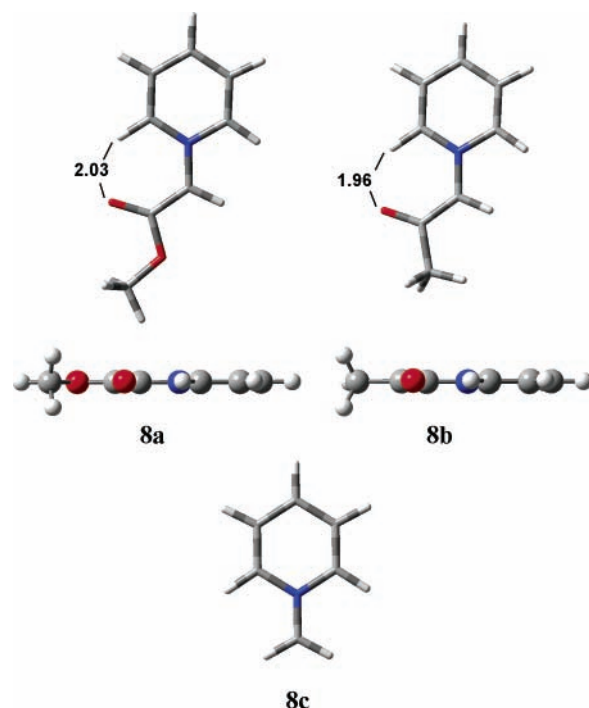


FIGURE 6. B3LYP/6-311G\*\* optimized geometries of **8a–c** illustrating coplanar orientation of the pyridine ring and the ylidic carbon.

$\text{PCl}_2$  moiety as obtained from second-order perturbation analysis. It has been demonstrated previously that the second-order perturbation approach has parallel and comparable trends with the Fock matrix deletion approach and can be used efficiently to study the relative importance of various individual delocalizations in a molecule.<sup>36,37,39,56</sup> An analysis of the donor–acceptor interactions present in different rotamers of various ylides under investigation indicates that on the basis of localized NBOs there can be two categories of molecules: (i) represented by the Lewis structure having a ylidic charge on C7 in the form of a lone pair as in **5a<sub>M1</sub>**, **5b<sub>M1</sub>**, **5e**, **6<sub>M1</sub>**, **8a**, and **8b** and (ii) including **5a<sub>M2</sub>**, **5a<sub>TS</sub>**, **5b<sub>M2</sub>**, **5b<sub>TS</sub>**, **5c**, and **5d** and denoted by a Lewis structure having a formal double bond between C7 and the phosphorus atom resulting from the (C7) $p\pi$ –(P) $d\pi$  overlap characterized by the presence of the  $\pi_{\text{C7-P}}$  NBO having a significant contribution of the phosphorus  $d$  orbital. It is also observed that this  $n_{\text{C7}}$  or  $\pi_{\text{C7-P}}$  NBO having the highest energy and the smallest occupancy (Table 2) is the one that is associated with the most significant donor–acceptor interactions in each case. In the absence of the  $\text{PCl}_2$  group in the pyridinium methylides **8a** and **8b**, the  $\text{C}_{\text{ylidic}}$  lone pair overlaps with only two vicinal antibonding orbitals, namely,  $\pi^*_{\text{C1-N6}}$  and  $\pi^*_{\text{C8-O9}}$ , leading to the extended conjugation in both directions with high delocalization energies (87–121 kcal/mol), consequently resulting in a perfectly coplanar orientation of the pyridinium ring and the ylidic carbon. Stabilization energies of these two conjugative interactions, i.e.,  $n_{\text{C}_{\text{ylidic}}} \rightarrow \pi^*_{\text{C1-N6}}$  and  $n_{\text{C}_{\text{ylidic}}} \rightarrow \pi^*_{\text{C8-O9}}$ , are quite large in **6<sub>M1</sub>** and **6<sub>M2</sub>** also; the presence of an insignificant amount of stabilization energies of negative hyperconjugative  $n_{\text{C}_{\text{ylidic}}} \rightarrow \sigma^*_{\text{P-H}}$  interactions and an orthogonal arrangement of lone pairs at C7 and phosphorus (Figure 3) again result in a coplanar orientation of the two moieties. However, in the case of **5a<sub>M1</sub>** and **5b<sub>M1</sub>**, the unsymmetrical orientation of

(54) Bondi, A. J. *Phys. Chem.* **1964**, *68*, 441.

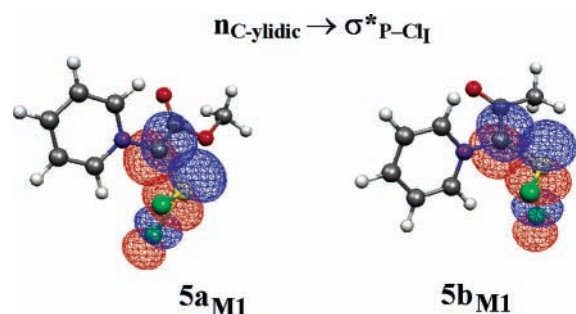
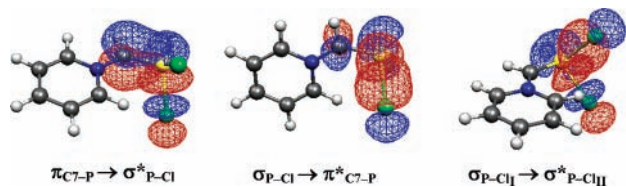
(55) Second-order stabilization energy estimated by:  $\Delta E_{ij} = q_i \{ F_{ij}^2 / (\epsilon_i - \epsilon_j) \}$  where  $q_i$  is the occupancy of donor orbital  $i$  from which the electrons are donated to orbital  $j$ ,  $\epsilon_i$  and  $\epsilon_j$  are orbital energies, and  $F_{ij}$  is the off-diagonal NBO Fock matrix element.

(56) Alabugin, I. V.; Zeidan, T. A. *J. Am. Chem. Soc.* **2002**, *124*, 3175.

**TABLE 2.** Second-Order Perturbation Energies ( $E_{ij}$  in kcal/mol) of Main Delocalizing Interactions Associated with the Ylidic Moiety in Pyridinium Methyldes **5**, **6**, and **8** Calculated from NBO Analyses at the B3LYP/6-311++G\*\* Level

| donor→acceptor                                     | <b>5a<sub>M1</sub></b> | <b>5a<sub>M2</sub></b> | <b>5a<sub>TS</sub></b> | <b>5b<sub>M1</sub></b> | <b>5b<sub>M2</sub></b> | <b>5b<sub>TS</sub></b> | <b>5c</b> | <b>5d</b> | <b>5e</b> | <b>6<sub>M1</sub><sup>a</sup></b> | <b>6<sub>M2</sub><sup>a</sup></b> | <b>8a</b> | <b>8b</b> |
|--|------------------------|------------------------|------------------------|------------------------|------------------------|------------------------|-----------|-----------|-----------|-----------------------------------|-----------------------------------|-----------|-----------|
| $n_{C7} \rightarrow \sigma^*_{P-Cl_I}$             | 30.09                  |                        |                        | 31.46                  |                        |                        |           |           | 2.82      | 4.84                              | 3.26                              |           |           |
| $n_{C7} \rightarrow \sigma^*_{P-Cl_{II}}$          | 6.36                   |                        |                        | 7.74                   |                        |                        |           |           | 28.40     | 3.91                              | 5.24                              |           |           |
| $n_{C7} \rightarrow \pi^*_{C1-N6}$                 | 43.41                  |                        |                        | 28.37                  |                        |                        |           |           | 4.40      | 99.20                             | 86.04                             | 121.42    | 109.68    |
| $n_{C7} \rightarrow \pi^*_{C8-O9}$                 | 77.60                  |                        |                        | 68.68                  |                        |                        |           |           |           | 87.59                             | 89.31                             | 96.14     | 87.10     |
| $\pi_{C7-P} \rightarrow \sigma^*_{P-Cl_I}$         |                        | 18.49                  | 33.96                  |                        | 18.15                  | 31.56                  | 28.47     | 30.11     |           |                                   |                                   |           |           |
| $\pi_{C7-P} \rightarrow \sigma^*_{P-Cl_{II}}$      |                        | 22.32                  | 8.83                   |                        | 27.38                  | 14.89                  | 28.37     | 18.95     |           |                                   |                                   |           |           |
| $\pi_{C7-P} \rightarrow \pi^*_{C5-N6}$             |                        | 35.05                  | 23.30                  |                        | 21.28                  | 16.42                  | 47.67     | 39.54     |           |                                   |                                   |           |           |
| $\pi_{C7-P} \rightarrow \pi^*_{C8-O9}$             |                        | 57.30                  | 60.09                  |                        | 51.51                  | 60.15                  |           |           |           |                                   |                                   |           |           |
| $\sigma_{P-Cl_I} \rightarrow \pi^*_{C7-P}$         | 1.61                   | 68.28                  | 119.74                 |                        | 52.05                  | 106.10                 | 64.87     | 93.95     |           |                                   |                                   |           |           |
| $\sigma_{P-Cl_{II}} \rightarrow \pi^*_{C7-P}$      | 1.23                   | 80.56                  | 37.04                  |                        | 89.51                  | 55.07                  | 64.46     | 40.15     |           |                                   |                                   |           |           |
| $\sigma_{P-Cl_I} \rightarrow \sigma^*_{P-Cl_{II}}$ | 0.91                   | 34.50                  | 8.07                   | 1.02                   | 30.25                  | 13.29                  | 33.93     | 29.46     | 0.90      | 1.09                              | 0.94                              |           |           |
| $\sigma_{P-Cl_{II}} \rightarrow \sigma^*_{P-Cl_I}$ | 0.82                   | 32.44                  | 10.00                  | 1.02                   | 32.75                  | 15.02                  | 33.97     | 28.83     | 0.75      | 1.10                              | 0.94                              |           |           |
| occupancy <sup>b</sup>                             | 1.435                  | 1.563                  | 1.569                  | 1.422                  | 1.576                  | 1.569                  | 1.576     | 1.599     | 1.640     | 1.342                             | 1.360                             | 1.281     | 1.271     |
| energy (au) <sup>b</sup>                           | -0.1768                | -0.1990                | -0.1897                | -0.1765                | -0.2006                | -0.1891                | -0.2009   | -0.2268   | -0.2438   | -0.1500                           | -0.1468                           | -0.1375   | -0.1369   |

<sup>a</sup> Data for P–H bonds in place of P–Cl. <sup>b</sup> Occupancy in electrons and energy of lone pair NBO at C7 in **5a<sub>M1</sub>**, **5b<sub>M1</sub>**, **5e**, **6<sub>M1</sub>**, **8a**, and **8b** or BD(2) NBO at C7–P in **5a<sub>M2</sub>**, **5a<sub>TS</sub>**, **5b<sub>M2</sub>**, **5b<sub>TS</sub>**, **5c**, and **5d**.

**FIGURE 7.** Graphical representation of the NBO orbital overlap corresponding to the  $n_{C_{ylidic}} \rightarrow \sigma^*_{P-Cl_I}$  negative hyperconjugative interaction in **5a<sub>M1</sub>** and **5b<sub>M1</sub>**.**FIGURE 8.** Graphical representation of selected NBO orbital overlaps corresponding to negative hyperconjugative and hyperconjugative interactions in **5c**.

the  $-PCl_2$  group facilitates the overlap of the ylidic charge with one antibonding P–Cl orbital (Figure 7) resulting in the negative hyperconjugative  $n_{C_{ylidic}} \rightarrow \sigma^*_{P-Cl_I}$  interaction of significant stabilization energy (30–31.5 kcal/mol); a substantial decrease in  $n_{C_{ylidic}} \rightarrow \pi^*_{C1-N6}$  conjugation (by  $\sim 80$  kcal/mol as compared to **8a** and **8b**) is accompanied by loss of coplanarity of the ylidic carbon with the pyridinium ring.

In the case of unsubstituted pyridinium dichlorophosphino-methylide **5c** (Figure 8), having a ylidic charge localized in the form of a  $\pi_{C7-P}$  NBO, hyperconjugative  $\sigma_{P-Cl_I} \rightarrow \pi^*_{C7-P}$  and  $\sigma_{P-Cl_I} \rightarrow \sigma^*_{P-Cl_I}$  interactions are also present, which are more effective than the negative hyperconjugative  $\pi_{C7-P} \rightarrow \sigma^*_{P-Cl_I}$  interactions in terms of the stabilization energies. It is remarkable to note that each one of these three types of interactions with either of the two P–Cl bonds is of the same order (Table 2), confirming the symmetrical disposition of the  $-PCl_2$  moiety around the plane of the ylidic carbon and the pyridine ring.

A comparison of the various hyperconjugative and negative hyperconjugative, i.e.,  $\sigma_{P-Cl_I} \rightarrow \pi^*_{C7-P}$ ,  $\sigma_{P-Cl_I} \rightarrow \sigma^*_{P-Cl_I}$ , and  $\pi_{C7-P} \rightarrow \sigma^*_{P-Cl_I}$ , interactions in **5a<sub>M2</sub>**, **5a<sub>TS</sub>**, **5b<sub>M2</sub>**, and **5b<sub>TS</sub>** (Table

2) reveals that the  $\sigma_{P-Cl_I} \rightarrow \pi^*_{C7-P}$  interaction (having a large stabilization energy of 106.1–119.7 kcal/mol) in transition structures **5a<sub>TS</sub>** and **5b<sub>TS</sub>** plays an important role and results in the elongation of the P–Cl<sub>I</sub> bond.

## Conclusions

The present study indicates that the substituent-dependent anomeric effects play an important role in deciding conformational preferences of the pyridinium methyldes exhibiting deviations from the orthogonal arrangement of lone pairs. Ylidic carbon substituents that allow significant delocalization of the ylidic charge into the pyridine ring result in a coplanar orientation, and the increased delocalization of the ylidic charge to the substituents in the form of  $n \rightarrow \sigma^*$  negative hyperconjugative,  $n \rightarrow \pi^*$  conjugative, or  $\sigma \rightarrow \pi^*$  hyperconjugative interactions reduces the extent of the charge donation to the pyridinium ring causing deviation from coplanarity. The existence of a particular conjugative or hyperconjugative interaction, reflected by changes in bond lengths and angles, can be well assessed from donor–acceptor energies and NBO overlaps calculated from natural bond orbital analyses. In view of the importance of structural and electronic features in the stable conformation of a molecule in deciding its reactivity trends, the extension of the present study may help in evaluating the role of more substituent-dependent stereoelectronic effects in controlling the stability of a particular conformation.

**Acknowledgment.** Financial support from the Department of Science and Technology, Government of India, New Delhi (Project Grant – SR/FTP/CS-115/2001), is gratefully acknowledged. We thank Professor R. K. Bansal for inspirational discussions. K.K.S. thanks CSIR, New Delhi, for a junior research fellowship.

**Supporting Information Available:** The total energies of **5**, **6**, **7**, and **8** calculated at the B3LYP/6-311G\*\*//B3LYP/6-311G\*\* and B3LYP/6-311++G\*\*//B3LYP/6-311G\*\* levels. Selected structural parameters obtained from the optimized geometries. Cartesian coordinates of the B3LYP/6-311G\*\* optimized geometries of **5**, **6**, **7**, and **8** in the gas phase and of **5a** in toluene and dichloromethane. This material is available free of charge via the Internet at <http://pubs.acs.org>.

JO051852Q